PRECISION MEASUREMENT OF THE HIGGS BOSON MASS AND SEARCH FOR DILEPTON MASS RESONANCES IN $H \rightarrow 4\ell$ DECAYS USING THE CMS DETECTOR AT THE LHC

By

JAKE ROSENZWEIG

A DISSERTATION PRESENTED TO THE GRADUATE SCHOOL
OF THE UNIVERSITY OF FLORIDA IN PARTIAL FULFILLMENT
OF THE REQUIREMENTS FOR THE DEGREE OF
DOCTOR OF PHILOSOPHY

UNIVERSITY OF FLORIDA

2022

This work is dedicated to the living and loving memory of Jacob Myhre.

ACKNOWLEDGEMENTS

Without so many two- and four-legged blessings along the way, I could never have made it to this point in my academic career. Thus, I begin by giving my endless gratitude to my high energy physics mentors, Professors Andrey Korytov and Guenkah Mitselmakher, for granting me this one-of-a-kind opportunity to do real *science* at CERN.

To my wife, Suzanne Rosenzweig, for showing me that dreams *do* come true. To my mother and father, Vicki and John, who always reassured me that I could achieve anything I put my mind to. Sleep peacefully, Mom. To my siblings, Alex, Ryan, Devin, Jace, and Claudia who frequently and gently reminded me that life existed outside of grad school. To Auntie Rachel and Uncle Yuri, who just *get* me and have given to me everything I could have possible asked for. To my mentor, Sheldon Friedman, and his wife, Rita Friedman (Rosenzweig), who chose to invest in my success at a young age. I have only made it this far thanks to their undying encouragement, love, and optimism. To Sheldon's best friend, Dr. Bernard Khoury, whose reputation and has helped pave my own path. To the many moms who generously gave unconditional support during the darkest of times and unequivocal love during the brightest times: Cyndi Reilly-Rogers, Dawn Hood, Margaret Sherrill, and Silet Wiley.

To Dr. Filippo Errico for his focus, leadership, selflessness, and patience in leading the Higgs mass analysis. To Dr. Lucien Lo for showing me the simplicity and beauty of Python in his typical laid-back way and for leading the dilepton analysis. To Dr. Noah Steinberg for showing me how majestically physics can be communicated from mind to mind. To Dr. Darin Acosta, for spending many hours of physics discussion with me and the other students, who have helped us build our "CMS Office Hours" Ari Gonzalez, Cris Caballeros, Jeremiah Anglin, Sean Kent, Evan Koenig, Neha Rawal, Nik Menendez, John Rötter. To the gents who paved my way to and through the world of CMS, Brendan Regnery and Bhargav Joshi. To my mentee, Matthew Dittrich, for accepting the baton of knowledge and making everything come full circle.

To my comrades for showing me what it takes to survive the core courses, Dr. Atool Divakarla, Dr. Brien O'Brendan, Dr. Donyell Guerrero, and Dr. Vladinar Martinez. To Adamya Goyal for all his gentleness, humility, patience, and tutorage. To my Polish roommates in Saint-Genis-Pouilly for showing me what home away from home feels like: Bartoszek, Dziadziuś,

Karolina, and Sandruśa. To the boys who have been there since the beginning: Jish, Willis, The Shane, Zacman, Duck, and Marcus for their clever competition and continual camaraderie which has shaped me to this day.

To Big Tree who stood as a symbol of strength, beauty, and life for centuries before us. As Irma's wild whirring winds worsened, the cacophony of ripping roots resounded throughout the western corridor. There I stood in that frozen moment—awestruck, speechless—watching her *fall* helplessly towards the physics building. What could have been a catastrophe of cataclysmic proportions was instead a gentle grazing against the north windows of NPB where, there, she was gracefully laid to rest.

Finally, to Existence, for this unpredictable, unbelievable blip of an experience called Life.

TABLE OF CONTENTS

LIST OF TABLES

LIST OF FIGURES

Abstract of Dissertation Presented to the Graduate School
of the University of Florida in Partial Fulfillment of the
Requirements for the Degree of Doctor of Philosophy

PRECISION MEASUREMENT OF THE HIGGS BOSON MASS AND SEARCH FOR DILEPTON MASS RESONANCES IN $\mathrm{H} \to 4\ell$ DECAYS USING THE CMS DETECTOR AT THE LHC

By

Jake Rosenzweig

December 2022

Chair: Andrey Korytov
Co-Chair: Guenakh Mitselmakher
Major: Physics

The mass of the Higgs boson is measured in the $\mathrm{H} \to \mathrm{ZZ}^* \to 4\ell$ ($\ell = \mathrm{e}, \mu$) decay channel and is found to be $m_{\mathrm{H}} = 125.38 \pm 0.11\,\mathrm{GeV}$; the most precise measurement of m_{H} in the world to date. The data for the measurement were produced from proton-proton (pp) collisions at the Large Hadron Collider with a center-of-mass energy of 13 TeV during Run 2 (2016–2018), corresponding to an integrated luminosity of $137.1\,\mathrm{fb}^{-1}$, and were collected by the Compact Muon Solenoid experiment. This measurement uses an improved analysis technique in which the final state muon tracks are constrained to originate from the primary pp vertex. Using data sets from the same run, a search for low-mass dilepton resonances in Higgs boson decays to the 4ℓ final state is also conducted. No significant deviation from the Standard Model prediction is observed.

CHAPTER 1

HIGGS BOSON MASS MEASUREMENT IN THE $H \rightarrow ZZ^{*} \rightarrow 4\ell$ CHANNEL

1.1 Motivation

When the CMS and ATLAS collaborations announced the discovery of the Higgs boson on July 4, 2012, this was a momentous achievement in particle physics because the so-called "missing" piece of the SM was found. Evidence of the Higgs boson's existence also motivates the associated Higgs field, which permeates all of spacetime and explains the origins of the masses of all the other massive fundamental particles (Chapter **??**).

The Higgs boson is interesting for a variety of reasons. First, it is currently one of a kind—the only fundamental scalar particle ever discovered at the time of this writing. Second, the mass of the Higgs boson theoretically determines the stability of our very Universe (Fig. **??**). Third, the unique boson could be a portal to new physics—i.e., physics beyond the Standard Model (BSM)—e.g., by decaying into BSM low-mass dilepton mass resonances (Chapter **??**). Fourth, the Higgs boson may not be the only one of its kind; some BSM models theorize that other kinds of Higgs bosons may exist. Fifth, *are we certain that the Higgs boson discovered in 2012 is the same as the one predicted by the SM?* To check this, it is necessary to compare the Higgs boson's measured properties to its predicted ones. One such property is the mass of the Higgs boson (m_{H}).

This chapter details the measurement of m_{H} full Run 2 data from the LHC as analyzed by the CMS detector. Although many previous measurements of m_{H} have already been made (e.g., by the ATLAS and CMS collaborations as shown in Fig. 1-1), the measurement presented in this dissertation gives the world's most precise value of m_{H}.

First, a general overview of the logic and analysis workflow for the m_{H} measurement is motivated in Sec. **??**. The specific data sets, simulated samples, and triggers used in the analysis are then detailed in Sec. 1.2. Then the event reconstruction and event selection are described in Sec. 1.3. Afterwards, an analysis of the background estimation is given in Sec. **??**. The signal modeling and improvements utilized in this measurement are then laid out, which include the kinematic discriminant, per-event mass uncertainties, and the vertex constraint in Sec. 1.4. A treatment of the systematic uncertainties follows in Sec. **??**. The chapter concludes with a summary of the m_{H} measurement results in Sec. **??**.

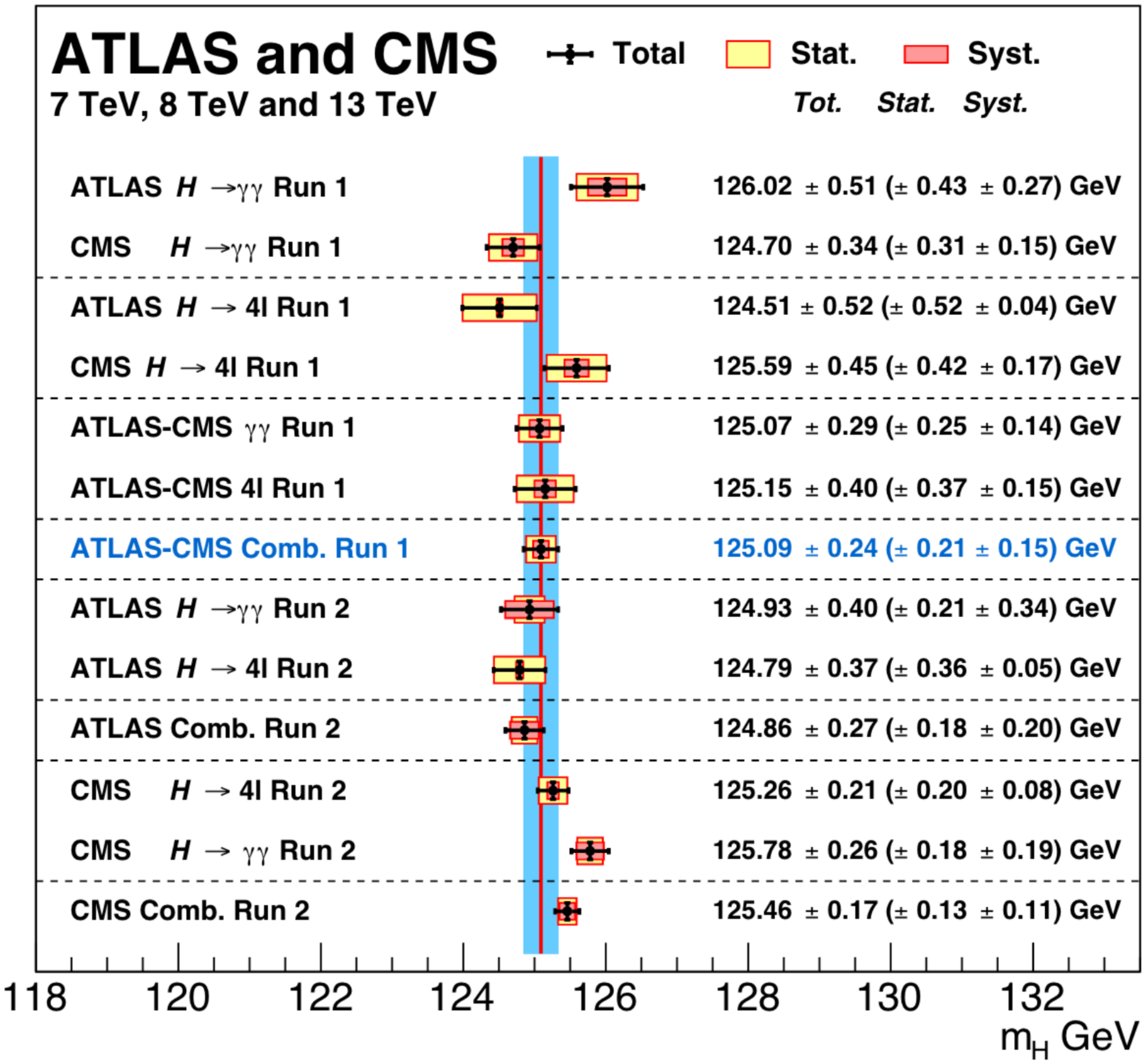

Figure 1-1. Various measurements of m_{H} made by the CMS and ATLAS collaborations in the $\mathrm{H} \rightarrow \gamma\gamma$ and $\mathrm{H} \rightarrow \mathrm{ZZ}^{*} \rightarrow 4\ell$ channels, in Runs 1 and 2 of the LHC. Plot taken from [1].

1.2 Analyzed Data

The CMS experiment recorded LHC **??** data during 2016, 2017, and 2018 (collectively called Run 2), corresponding to an integrated luminosity of $137.1\,\mathrm{fb}^{-1}$. These events were categorized by the trigger system **??** into different data sets, depending on which triggers "fired", i.e., whether the event passed the trigger criteria or not. The names of the data sets are listed in Tables 1-4–1-6 and follow the format `/object_type/campaign/datatier`. This analysis uses the ultra legacy (UL) reconstruction []. It should be noted that the 2016 data are split into 2 different reconstruction versions, starting at Run2016F: the first version is "pre-VFP", which uses HIP mitigation (HIPM) in the reconstruction, and the second is "post-VFP", which uses the default reconstruction.

For the $\mathrm{H} \to \mathrm{ZZ}^* \to 4\ell$ analysis, Sec. 1.2.1 lists the triggers used, Sec. 1.2.2 details the data sets used, and Sec. 1.2.3 summarizes the simulated samples used.

1.2.1 Triggers

1.2.2 Data Sets

1.2.3 Simulated Events

The data set names containing the simulated events for signal and background processes are listed in Tables 1-7–1-9.

1.2.4 PileUp reweight

Simulated samples are reweighted taking into account pileUp distribution. PileUp weight is extracted for each year matching simulation and data distribution. The minimum bias cross-section used for each year is 69.2 mb. PileUp distributions for each year are shown in Fig. 1-2.

Table 1-1. Trigger paths used to collect 2016 data (pre- and post-VFP) for the measurement of m_{H}.

HLT path	Prescale	Primary data set
HLT_DoubleEle33_CaloIdL_GsfTrkIdVL_v*	1	DoubleEG
HLT_Ele16_Ele12_Ele8_CaloIdL_TrackIdL_v*	1	DoubleEG
HLT_Ele17_Ele12_CaloIdL_TrackIdL_IsoVL_DZ_v*	1	DoubleEG
HLT_Ele23_Ele12_CaloIdL_TrackIdL_IsoVL_DZ_v*	1	DoubleEG
HLT_Mu17_TrkIsoVVL_Mu8_TrkIsoVVL_DZ_v*	1	DoubleMuon
HLT_Mu17_TrkIsoVVL_Mu8_TrkIsoVVL_v*	1	DoubleMuon
HLT_Mu17_TrkIsoVVL_TkMu8_TrkIsoVVL_DZ_v*	1	DoubleMuon
HLT_Mu17_TrkIsoVVL_TkMu8_TrkIsoVVL_v*	1	DoubleMuon
HLT_TripleMu_12_10_5_v*	1	DoubleMuon
HLT_DiMu9_Ele9_CaloIdL_TrackIdL_v*	1	MuonEG
HLT_Mu8_DiEle12_CaloIdL_TrackIdL_v*	1	MuonEG
HLT_Mu8_TrkIsoVVL_Ele17_CaloIdL_TrackIdL_IsoVL_v*	1	MuonEG
HLT_Mu8_TrkIsoVVL_Ele23_CaloIdL_TrackIdL_IsoVL_DZ_v*	1	MuonEG
HLT_Mu8_TrkIsoVVL_Ele23_CaloIdL_TrackIdL_IsoVL_v*	1	MuonEG
HLT_Mu17_TrkIsoVVL_Ele12_CaloIdL_TrackIdL_IsoVL_v*	1	MuonEG
HLT_Mu23_TrkIsoVVL_Ele8_CaloIdL_TrackIdL_IsoVL_v*	1	MuonEG
HLT_Mu23_TrkIsoVVL_Ele12_CaloIdL_TrackIdL_IsoVL_DZ_v*	1	MuonEG
HLT_Mu23_TrkIsoVVL_Ele12_CaloIdL_TrackIdL_IsoVL_v*	1	MuonEG
HLT_Ele25_eta2p1_WPTight_Gsf_v*	1	SingleElectron
HLT_Ele27_eta2p1_WPLoose_Gsf_v*	1	SingleElectron
HLT_Ele27_WPTight_Gsf_v*	1	SingleElectron
HLT_Ele32_eta2p1_WPTight_Gsf_v*	1	SingleElectron
HLT_IsoMu20_v* OR HLT_IsoTkMu20_v*	1	SingleMuon
HLT_IsoMu22_v* OR HLT_IsoTkMu22_v*	1	SingleMuon
HLT_IsoMu24_v* OR HLT_IsoTkMu24_v*	1	SingleMuon

Table 1-2. Trigger paths used to collect 2017 data for the measurement of m_{H}.

HLT path	Prescale	Primary data set
HLT_DoubleEle33_CaloIdL_MW_v*	1	DoubleEG
HLT_Ele16_Ele12_Ele8_CaloIdL_TrackIdL_v*	1	DoubleEG
HLT_Ele23_Ele12_CaloIdL_TrackIdL_IsoVL_v*	1	DoubleEG
HLT_Mu17_TrkIsoVVL_Mu8_TrkIsoVVL_DZ_Mass3p8_v*	1	DoubleMuon
HLT_Mu17_TrkIsoVVL_Mu8_TrkIsoVVL_DZ_Mass8_v*	1	DoubleMuon
HLT_TripleMu_10_5_5_DZ_v*	1	DoubleMuon
HLT_TripleMu_12_10_5_v*	1	DoubleMuon
HLT_DiMu9_Ele9_CaloIdL_TrackIdL_DZ_v*	1	MuonEG
HLT_Mu8_DiEle12_CaloIdL_TrackIdL_DZ_v*	1	MuonEG
HLT_Mu8_DiEle12_CaloIdL_TrackIdL_v*	1	MuonEG
HLT_Mu8_TrkIsoVVL_Ele23_CaloIdL_TrackIdL_IsoVL_DZ_v*	1	MuonEG
HLT_Mu12_TrkIsoVVL_Ele23_CaloIdL_TrackIdL_IsoVL_DZ_v*	1	MuonEG
HLT_Mu23_TrkIsoVVL_Ele12_CaloIdL_TrackIdL_IsoVL_DZ_v*	1	MuonEG
HLT_Mu23_TrkIsoVVL_Ele12_CaloIdL_TrackIdL_IsoVL_v*	1	MuonEG
HLT_Ele35_WPTight_Gsf_v*	1	SingleElectron
HLT_Ele38_WPTight_Gsf_v*	1	SingleElectron
HLT_Ele40_WPTight_Gsf_v*	1	SingleElectron
HLT_IsoMu27_v*	1	SingleMuon

Table 1-3. Trigger paths used to collect 2018 data for the measurement of m_{H}.

HLT path	Prescale	Primary data set
HLT_DoubleEle25_CaloIdL_MW_v*	1	DoubleEG
HLT_Ele23_Ele12_CaloIdL_TrackIdL_IsoVL_v*	1	DoubleEG
HLT_Mu17_TrkIsoVVL_Mu8_TrkIsoVVL_DZ_Mass3p8_v*	1	DoubleMuon
HLT_TripleMu_10_5_5_DZ_v*	1	DoubleMuon
HLT_TripleMu_12_10_5_v*	1	DoubleMuon
HLT_DiMu9_Ele9_CaloIdL_TrackIdL_DZ_v*	1	MuonEG
HLT_Mu8_DiEle12_CaloIdL_TrackIdL_DZ_v*	1	MuonEG
HLT_Mu8_DiEle12_CaloIdL_TrackIdL_v*	1	MuonEG
HLT_Mu8_TrkIsoVVL_Ele23_CaloIdL_TrackIdL_IsoVL_DZ_v*	1	MuonEG
HLT_Mu12_TrkIsoVVL_Ele23_CaloIdL_TrackIdL_IsoVL_DZ_v*	1	MuonEG
HLT_Mu23_TrkIsoVVL_Ele12_CaloIdL_TrackIdL_IsoVL_DZ_v*	1	MuonEG
HLT_Mu23_TrkIsoVVL_Ele12_CaloIdL_TrackIdL_IsoVL_v*	1	MuonEG
HLT_Ele32_WPTight_Gsf_v*	1	SingleElectron
HLT_IsoMu24_v*	1	SingleMuon

Table 1-4. Names of the UL 2016 data sets and the corresponding integrated luminosities ($\mathcal{L}_{\text{int}}$).

Data set name	Integrated luminosity (fb^{-1})
/DoubleEG/Run2016B-ver1_HIPM_UL2016_MiniAODv2-v1/MINIAOD /DoubleMuon/Run2016B-ver1_HIPM_UL2016_MiniAODv2-v1/MINIAOD /SingleElectron/Run2016B-ver1_HIPM_UL2016_MiniAODv2-v2/MINIAOD /SingleMuon/Run2016B-ver1_HIPM_UL2016_MiniAODv2-v2/MINIAOD /MuonEG/Run2016B-ver1_HIPM_UL2016_MiniAODv2-v2/MINIAOD	TODO
/DoubleEG/Run2016B-ver2_HIPM_UL2016_MiniAODv2-v3/MINIAOD /DoubleMuon/Run2016B-ver2_HIPM_UL2016_MiniAODv2-v1/MINIAOD /SingleElectron/Run2016B-ver2_HIPM_UL2016_MiniAODv2-v2/MINIAOD /SingleMuon/Run2016B-ver2_HIPM_UL2016_MiniAODv2-v2/MINIAOD /MuonEG/Run2016B-ver2_HIPM_UL2016_MiniAODv2-v2/MINIAOD	TODO
/DoubleEG/Run2016C-HIPM_UL2016_MiniAODv2-v1/MINIAOD /DoubleMuon/Run2016C-HIPM_UL2016_MiniAODv2-v1/MINIAOD /SingleElectron/Run2016C-HIPM_UL2016_MiniAODv2-v2/MINIAOD /SingleMuon/Run2016C-HIPM_UL2016_MiniAODv2-v2/MINIAOD /MuonEG/Run2016C-HIPM_UL2016_MiniAODv2-v2/MINIAOD	TODO
/DoubleEG/Run2016D-HIPM_UL2016_MiniAODv2-v1/MINIAOD /DoubleMuon/Run2016D-HIPM_UL2016_MiniAODv2-v1/MINIAOD /SingleElectron/Run2016D-HIPM_UL2016_MiniAODv2-v2/MINIAOD /SingleMuon/Run2016D-HIPM_UL2016_MiniAODv2-v2/MINIAOD /MuonEG/Run2016D-HIPM_UL2016_MiniAODv2-v2/MINIAOD	TODO
/DoubleEG/Run2016E-HIPM_UL2016_MiniAODv2-v1/MINIAOD /DoubleMuon/Run2016E-HIPM_UL2016_MiniAODv2-v1/MINIAOD /SingleElectron/Run2016E-HIPM_UL2016_MiniAODv2-v5/MINIAOD /SingleMuon/Run2016E-HIPM_UL2016_MiniAODv2-v2/MINIAOD /MuonEG/Run2016E-HIPM_UL2016_MiniAODv2-v2/MINIAOD	TODO
/DoubleEG/Run2016F-HIPM_UL2016_MiniAODv2-v1/MINIAOD /DoubleMuon/Run2016F-HIPM_UL2016_MiniAODv2-v1/MINIAOD /SingleElectron/Run2016F-HIPM_UL2016_MiniAODv2-v2/MINIAOD /SingleMuon/Run2016F-HIPM_UL2016_MiniAODv2-v2/MINIAOD /MuonEG/Run2016F-HIPM_UL2016_MiniAODv2-v2/MINIAOD	TODO
/DoubleEG/Run2016F-UL2016_MiniAODv2-v1/MINIAOD /DoubleMuon/Run2016F-UL2016_MiniAODv2-v1/MINIAOD /SingleElectron/Run2016F-UL2016_MiniAODv2-v2/MINIAOD /SingleMuon/Run2016F-UL2016_MiniAODv2-v2/MINIAOD /MuonEG/Run2016F-UL2016_MiniAODv2-v2/MINIAOD	TODO
/DoubleEG/Run2016G-UL2016_MiniAODv2-v1/MINIAOD /DoubleMuon/Run2016G-UL2016_MiniAODv2-v1/MINIAOD /SingleElectron/Run2016G-UL2016_MiniAODv2-v2/MINIAOD /SingleMuon/Run2016G-UL2016_MiniAODv2-v2/MINIAOD /MuonEG/Run2016G-UL2016_MiniAODv2-v2/MINIAOD	TODO
/DoubleEG/Run2016H-UL2016_MiniAODv2-v1/MINIAOD /DoubleMuon/Run2016H-UL2016_MiniAODv2-v2/MINIAOD /SingleElectron/Run2016H-UL2016_MiniAODv2-v2/MINIAOD /SingleMuon/Run2016H-UL2016_MiniAODv2-v2/MINIAOD /MuonEG/Run2016H-UL2016_MiniAODv2-v2/MINIAOD	TODO

Table 1-5. Names of the UL 2017 data sets and the corresponding integrated luminosities ($\mathcal{L}_{\text{int}}$).

Data set name	Integrated luminosity (fb^{-1})
/SingleMuon/Run2017B-UL2017_MiniAODv2-v1/MINIAOD /SingleElectron/Run2017B-UL2017_MiniAODv2-v1/MINIAOD /DoubleMuon/Run2017B-UL2017_MiniAODv2-v1/MINIAOD /DoubleEG/Run2017B-UL2017_MiniAODv2-v1/MINIAOD /MuonEG/Run2017B-UL2017_MiniAODv2-v1/MINIAOD	TODO
/SingleMuon/Run2017C-UL2017_MiniAODv2-v1/MINIAOD /SingleElectron/Run2017C-UL2017_MiniAODv2-v1/MINIAOD /DoubleMuon/Run2017C-UL2017_MiniAODv2-v1/MINIAOD /DoubleEG/Run2017C-UL2017_MiniAODv2-v1/MINIAOD /MuonEG/Run2017C-UL2017_MiniAODv2-v1/MINIAOD	TODO
/SingleElectron/Run2017D-UL2017_MiniAODv2-v1/MINIAOD /SingleMuon/Run2017D-UL2017_MiniAODv2-v1/MINIAOD /DoubleMuon/Run2017D-UL2017_MiniAODv2-v1/MINIAOD /DoubleEG/Run2017D-UL2017_MiniAODv2-v1/MINIAOD /MuonEG/Run2017D-UL2017_MiniAODv2-v1/MINIAOD	TODO
/SingleElectron/Run2017E-UL2017_MiniAODv2-v1/MINIAOD /SingleMuon/Run2017E-UL2017_MiniAODv2-v1/MINIAOD /DoubleMuon/Run2017E-UL2017_MiniAODv2-v2/MINIAOD /DoubleEG/Run2017E-UL2017_MiniAODv2-v1/MINIAOD /MuonEG/Run2017E-UL2017_MiniAODv2-v1/MINIAOD	TODO
/SingleElectron/Run2017F-UL2017_MiniAODv2-v1/MINIAOD /SingleMuon/Run2017F-UL2017_MiniAODv2-v1/MINIAOD /DoubleMuon/Run2017F-UL2017_MiniAODv2-v1/MINIAOD /DoubleEG/Run2017F-UL2017_MiniAODv2-v1/MINIAOD /MuonEG/Run2017F-UL2017_MiniAODv2-v1/MINIAOD	TODO

Table 1-6. Names of the UL 2018 data sets and the corresponding integrated luminosities ($\mathcal{L}_{\text{int}}$).

Data set name	Integrated luminosity (fb^{-1})
/SingleMuon/Run2018A-UL2018_MiniAODv2-v3/MINIAOD /DoubleMuon/Run2018A-UL2018_MiniAODv2-v1/MINIAOD /EGamma/Run2018A-UL201_MiniAODv2-v1/MINIAOD /MuonEG/Run2018A-UL2018_MiniAODv2-v1/MINIAOD	TODO
/SingleMuon/Run2018B-UL2018_MiniAODv2-v2/MINIAOD /DoubleMuon/Run2018B-UL2018_MiniAODv2-v1/MINIAOD /EGamma/Run2018B-UL2018_MiniAODv2-v1/MINIAOD /MuonEG/Run2018B-UL2018_MiniAODv2-v1/MINIAOD	TODO
/SingleMuon/Run2018C-UL2018_MiniAODv2-v2/MINIAOD /DoubleMuon/Run2018C-UL2018_MiniAODv2-v1/MINIAOD /EGamma/Run2018C-UL2018_MiniAODv2-v1/MINIAOD /MuonEG/Run2018C-UL2018_MiniAODv2-v1/MINIAOD	TODO
/SingleMuon/Run2018D-UL2018_MiniAODv2-v3/MINIAOD /DoubleMuon/Run2018D-UL2018_MiniAODv2-v1/MINIAOD /EGamma/Run2018D-UL2018_MiniAODv2-v1/MINIAOD /MuonEG/Run2018D-UL2018_MiniAODv2-v1/MINIAOD	TODO

Table 1-7. Names of simulated signal and background samples for 2016 data.
[1] "RunIISummer20UL16MiniAODv2-106X_mcRun2_asymptotic_v17-v2/MINIAODSIM"
or
"RunIISummer20UL16MiniAODAPVv2-106X_mcRun2_asymptotic_preVFP_v11-v2/MINIAODSIM"

Name of signal data set	$\sigma \times \mathcal{B}$ (pb)
GluGluHToZZTo4L_M125_13TeV_powheg2_JHUGenV709_pythia8/[1]	0.01333521
VBF_HToZZTo4L_M125_13TeV_powheg2_JHUGenV709_pythia8/[1]	0.001038159
WplusH_HToZZTo4L_M125_13TeV_powheg2-minlo-HWJ_JHUGenV709_pythia8/[1]	0.0002305562
WminusH_HToZZTo4L_M125_13TeV_powheg2-minlo-HWJ_JHUGenV709_pythia8/[1]	0.0001462348
ZH_HToZZ_4LFilter_M125_13TeV_powheg2-minlo-HZJ_JHUGenV709_pythia8/[1]	0.0005321759
ttH_HToZZ_4LFilter_M125_13TeV_powheg2_JHUGenV709_pythia8/[1]	0.0003639351
bbH_HToZZTo4L_M125_13TeV_JHUgenV702_pythia8/[1]	0.0001339560
tqH_HToZZTo4L_M125_TuneCP5_13TeV-jhugenv7011pythia8/[1]	0.0000857830

Name of background data set	$\sigma \times \mathcal{B}$ (pb)
ZZTo4L_13TeV_powheg_pythia8/[1]	1.256
GluGluToContinToZZTo4e_13TeV_MCFM701_pythia8/[1]	0.00158549
GluGluToContinToZZTo4mu_13TeV_MCFM701_pythia8/[1]	0.00158549
GluGluToContinToZZTo4tau_13TeV_MCFM701_pythia8/[1]	0.00158549
GluGluToContinToZZTo2e2mu_13TeV_MCFM701_pythia8/[1]	0.0031942
GluGluToContinToZZTo2e2tau_13TeV_MCFM701_pythia8/[1]	0.0031942
GluGluToContinToZZTo2mu2tau_13TeV_MCFM701_pythia8/[1]	0.0031942

Table 1-8. Names of simulated signal and background samples for 2017 data.
[2] "RunIISummer20UL17MiniAODv2-106X_mc2017_realistic_v9/MINIAODSIM"

Name of signal data set	$\sigma \times \mathcal{B}$ (pb)
GluGluHToZZTo4L_M125_13TeV_powheg2_JHUGenV7011_pythia8/[2]	0.01333521
VBF_HToZZTo4L_M125_13TeV_powheg2_JHUGenV7011_pythia8/[2]	0.001038159
WplusH_HToZZTo4L_M125_13TeV_powheg2-minlo-HWJ_JHUGenV7011_pythia8/[2]	0.0002305562
WminusH_HToZZTo4L_M125_13TeV_powheg2-minlo-HWJ_JHUGenV7011_pythia8/[2]	0.0001462348
ZH_HToZZ_4LFilter_M125_13TeV_powheg2-minlo-HZJ_JHUGenV7011_pythia8/[2]	0.0005321759
ttH_HToZZ_4LFilter_M125_13TeV_powheg2_JHUGenV7011_pythia8/[2]	0.0003639351
bbH_HToZZTo4L_M125_13TeV_JHUGenV7011_pythia8/[2]	0.0001339560
tqH_HToZZTo4L_M125_TuneCP5_13TeV-jhugenv7011pythia8/[1]	0.0000857830

Name of background data set	$\sigma \times \mathcal{B}$ (pb)
ZZTo4L_13TeV_powheg_pythia8/[2]	1.256
GluGluToContinToZZTo4e_13TeV_MCFM701_pythia8/[2]	0.00158549
GluGluToContinToZZTo4mu_13TeV_MCFM701_pythia8/[2]	0.00158549
GluGluToContinToZZTo4tau_13TeV_MCFM701_pythia8/[2]	0.00158549
GluGluToContinToZZTo2e2mu_13TeV_MCFM701_pythia8/[2]	0.0031942
GluGluToContinToZZTo2e2tau_13TeV_MCFM701_pythia8/[2]	0.0031942
GluGluToContinToZZTo2mu2tau_13TeV_MCFM701_pythia8/[2]	0.0031942

Table 1-9. Names of simulated signal and background samples for 2018 data.
[3] “RunIISummer20UL18MiniAODv2-
106X_upgrade2018_realistic_v16_L1v1/MINIAODSIM”

Name of signal data set	$\sigma \times \mathcal{B}$ (pb)
GluGluHToZZTo4L_M125_13TeV_powheg2_JHUGenV7011_pythia8/[3]	0.01333521
VBF_HToZZTo4L_M125_13TeV_powheg2_JHUGenV7011_pythia8/[3]	0.001038159
WplusH_HToZZTo4L_M125_13TeV_powheg2-minlo-HWJ_JHUGenV7011_pythia8/[3]	0.0002305562
WminusH_HToZZTo4L_M125_13TeV_powheg2-minlo-HWJ_JHUGenV7011_pythia8/[3]	0.0001462348
ZH_HToZZ_4LFilter_M125_13TeV_powheg2-minlo-HZJ_JHUGenV7011_pythia8/[3]	0.0005321759
ttH_HToZZ_4LFilter_M125_13TeV_powheg2_JHUGenV7011_pythia8/[3]	0.0003639351
bbH_HToZZTo4L_M125_TuneCP2_13TeV-JHUGenV7011_pythia8/[3]	0.0001339560
tqH_HToZZTo4L_M125_TuneCP5_13TeV-jhugenv7011pythia8/[1]	0.0000857830

Name of background data set	$\sigma \times \mathcal{B}$ (pb)
ZZTo4L_TuneCP5_13TeV_powheg_pythia8/[3]	1.256
GluGluToContinToZZTo4e_13TeV_MCFM701_pythia8/[3]	0.00158549
GluGluToContinToZZTo4mu_13TeV_MCFM701_pythia8/[3]	0.00158549
GluGluToContinToZZTo4tau_13TeV_MCFM701_pythia8/[3]	0.00158549
GluGluToContinToZZTo2e2mu_13TeV_MCFM701_pythia8/[3]	0.0031942
GluGluToContinToZZTo2e2tau_13TeV_MCFM701_pythia8/[3]	0.0031942
GluGluToContinToZZTo2mu2tau_13TeV_MCFM701_pythia8/[3]	0.0031942

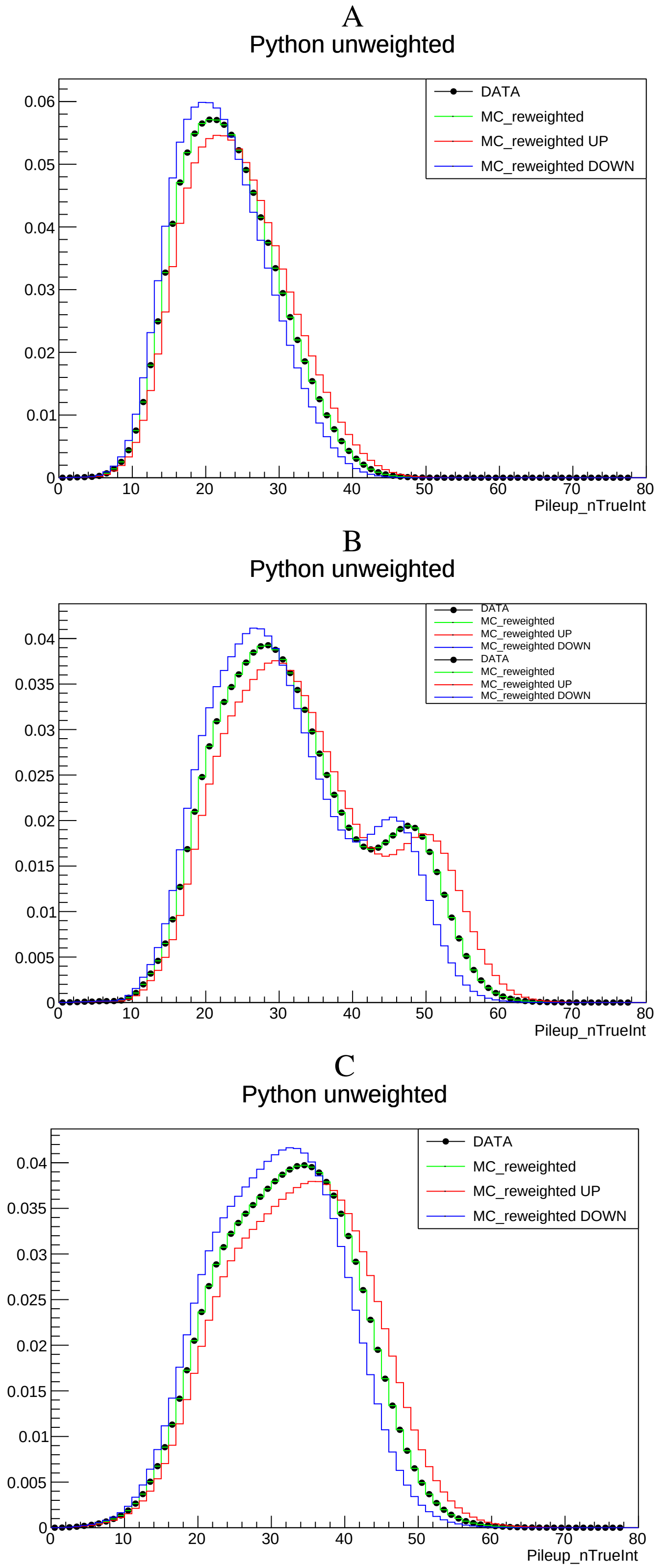

Figure 1-2. TODO:REWORD Data–simulation pileUp distributions: left 2016 (for pre and post-VFP), right 2017, bottom 2018. Up (down) scale has been obtained using 72.4 (66) mb.

1.3 Event Selection

Amidst the chaotic particle deluge that arises from pp collisions, events are carefully selected that appear to follow the decay chain and properties of the $\mathrm{H} \to \mathrm{ZZ}^* \to 4\ell$ signal. Crafting a well-designed *event selection* that identifies these signal events—while throwing away the non-signal events—is the goal. By implementing a rigorous trigger selection, vertex selection, final-state object selection, and ZZ-candidate selection, the purity of the signal process is optimized and, by extension, so is the precision on the measurement of m_{H}. The aforementioned selections are summarized in Ref. [**?**].

If an event contains more than one ZZ candidate that passes the selection criteria, then the candidate with the highest value of $\mathcal{D}^{\mathrm{kin}}_{\mathrm{bkg}}$ is selected as the overall ZZ candidate for the event.

After the full analysis selection is implemented in each of the 4ℓ final states, the expected and observed yields for the signal and background processes are given in Tables 1-10 and 1-11, which count events within the narrow signal region ($105 < m_{4\ell} < 140\,\mathrm{GeV}$) and wide signal region ($70 < m_{4\ell} < 170\,\mathrm{GeV}$), respectively.

Table 1-10. Number of expected and observed yields of signal and background processes within the narrow signal region $105 < m_{4\ell} < 140\,\mathrm{GeV}$ after the full event selection using $137.1\,\mathrm{fb}^{-1}$, split into the four final states.

Process	4μ	4e	2e2μ	2μ2e	Inclusive
$\mathrm{q\bar{q}} \to \mathrm{ZZ} \to 4\ell$	88.8	38.5	63.7	41.8	232.8
$\mathrm{gg} \to \mathrm{ZZ} \to 4\ell$	9.7	4.8	4.8	3.7	23.0
RB	32.4	12.2	29.2	18.6	92.4
Sum of Background	130.9	55.5	97.7	64.1	348.2
Signal ($m_{\mathrm{H}} = 125\,\mathrm{GeV}$)	90.5	48.2	64.6	53.0	256.3
Total Expected	221.4	103.7	162.3	117.1	604.5
Total Observed	—	—	—	—	—

Table 1-11. Number of expected and observed yields of signal and background processes within the wide signal region $70 < m_{4\ell} < 170\,\mathrm{GeV}$ after the full event selection using $137.1\,\mathrm{fb}^{-1}$, split into the four final states.

Process	4μ	$4e$	$2e2\mu$	$2\mu2e$	Inclusive
$q\bar{q} \to ZZ \to 4\ell$	486.7	192.0	246.0	170.1	1094.9
$gg \to ZZ \to 4\ell$	29.7	15.2	13.3	12.2	70.5
RB	70.1	30.3	61.5	42.2	204.1
Sum of Background	586.5	237.5	320.8	224.5	1369.3
Signal ($m_H = 125\,\mathrm{GeV}$)	92.4	49.6	66.5	54.3	262.8
Total Expected	679.0	287.2	387.4	278.8	1632.3
Total Observed	—	—	—	—	—

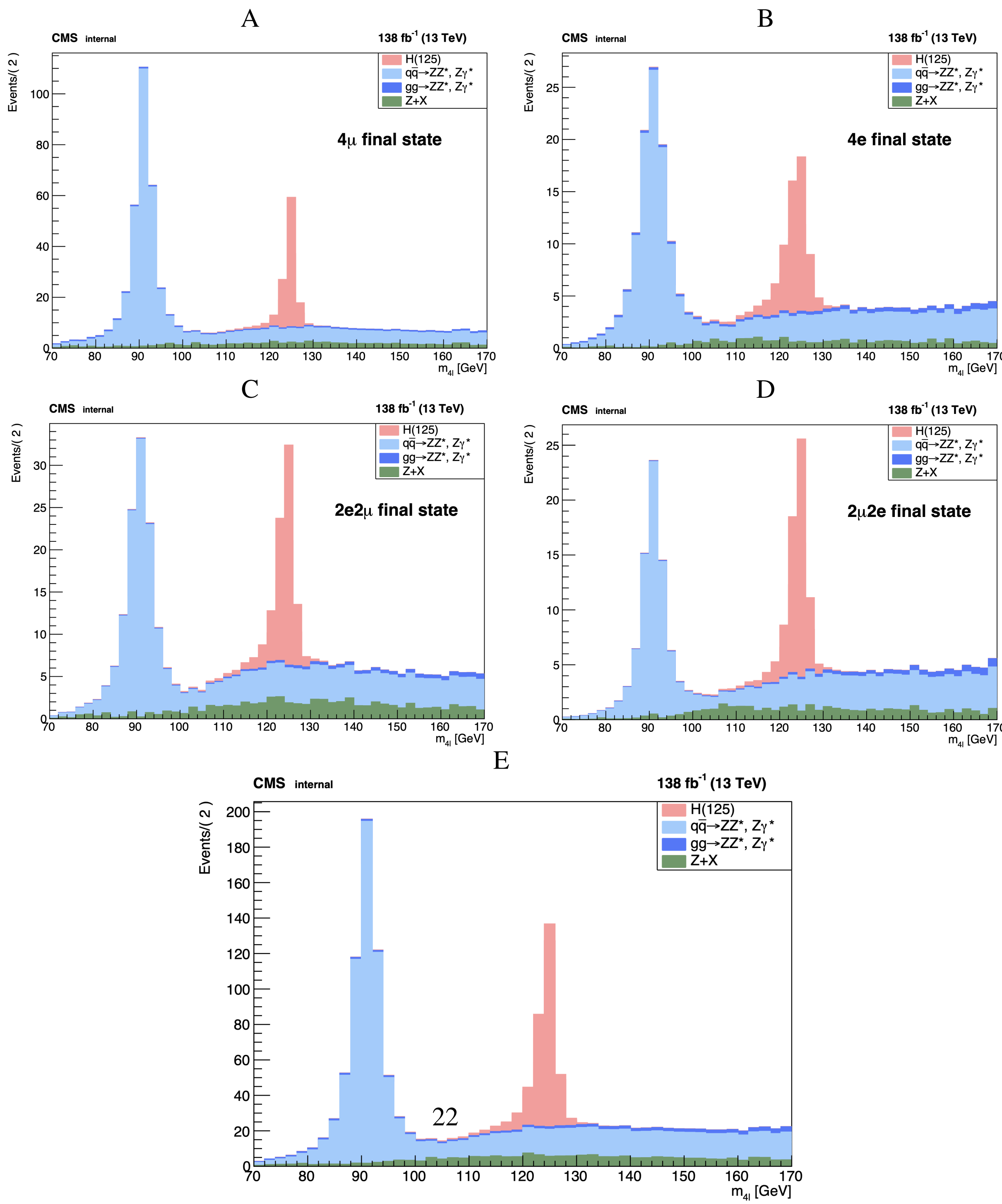

1.4 Signal Modeling

1.4.1 Signal Normalization

The normalization of the Higgs boson signal is obtained, from simulation, looking at the expected signal yields in the range [105, 140] GeV, for five simulated mass points (120, 124, 125, 126 and 130 GeV). A second order polynomial function is used to extract the dependence of the normalization from m_H. Fits are performed separately for each production mode, for each decay channel and for each year. Examples of the fits can be observed in Fig. 1-4

A

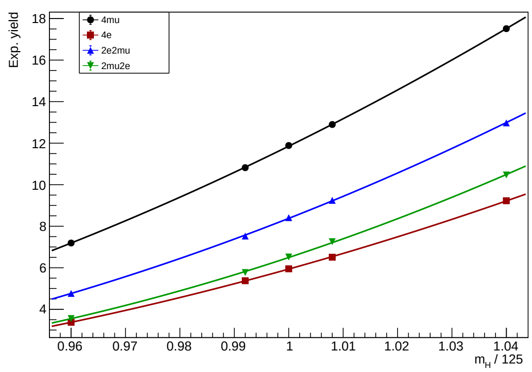

B

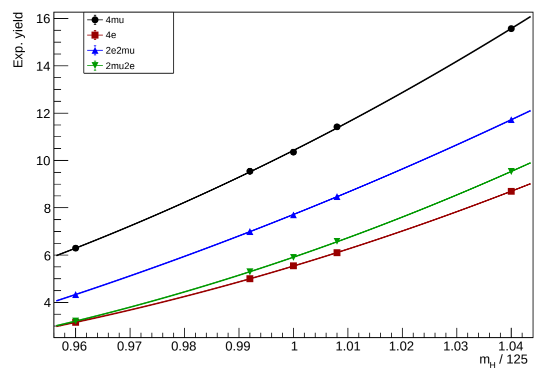

C

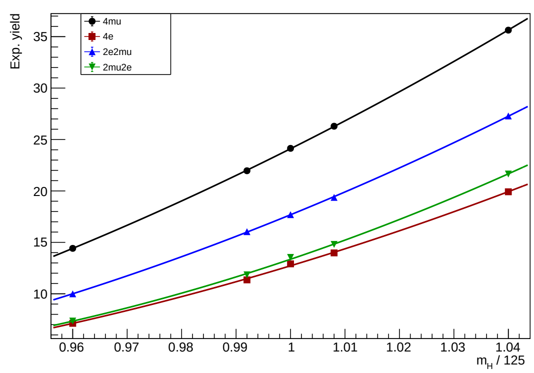

D

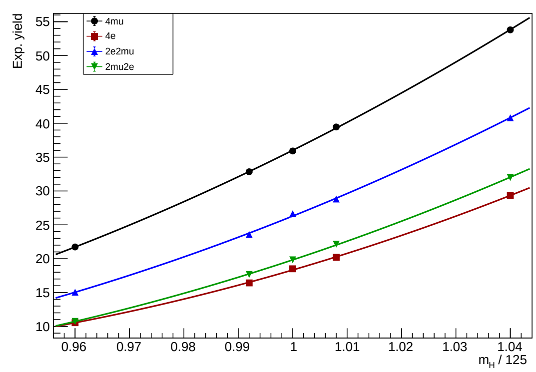

Figure 1-4. Normalization fit for ggH, in different decay channels, as a function of mass, for 2016 on top (pre-VFP on the left, post-VFP on the right), 2017 on bottom left, 2018 on the bottom right.

1.4.2 Parameterizing the Signal Mass Line Shape

The signal lineshape is obtained from the fit of the Higgs boson mass distribution, in the range [105, 140] GeV, using a double-sided Crystal Ball (DSCB) function, which has 6 parameters. Fit parameters are derived as a function of mass, using a first order polynomial:

$$param^i_{DSCB} = a^i + b^i\ (m_H - 125)$$

First, from the fit of the only 125 GeV sample, the “a” term for each parameter is extracted (“b” term in this case is not taken into account). Then, a second fit is performed: this time, “a” is fixed to the value found before, while “b” is kept free to float when fitting all five different mass points (120, 124, 126, 130 GeV, including 125 GeV sample) simultaneously.

The fit is performed separately, for each production mode, for each decay channel, in each year. To take into account the non-resonant contribution in the case of VH and ttH production modes, the DSCB is convoluted with a Landau function that describes the possibility for a lepton from the Higgs boson decay to be lost or not selected.

1.4.3 Building the 1D pdf

Higgs boson mass measurement is firstly extracted from a one-dimentional likelihood function $\mathcal{L}(m_{4\ell}|m_H)$, where m_H is fixed to the value of 125 GeV. The model and the normalisation used for the signal are described in 1.4.1.

As referece, Fig. 1-5 shows the four-lepton invariant mass distribution in the signal region ([105-140] GeV) using ggF events, with the DSCB fit for 2018, split in four different final states.

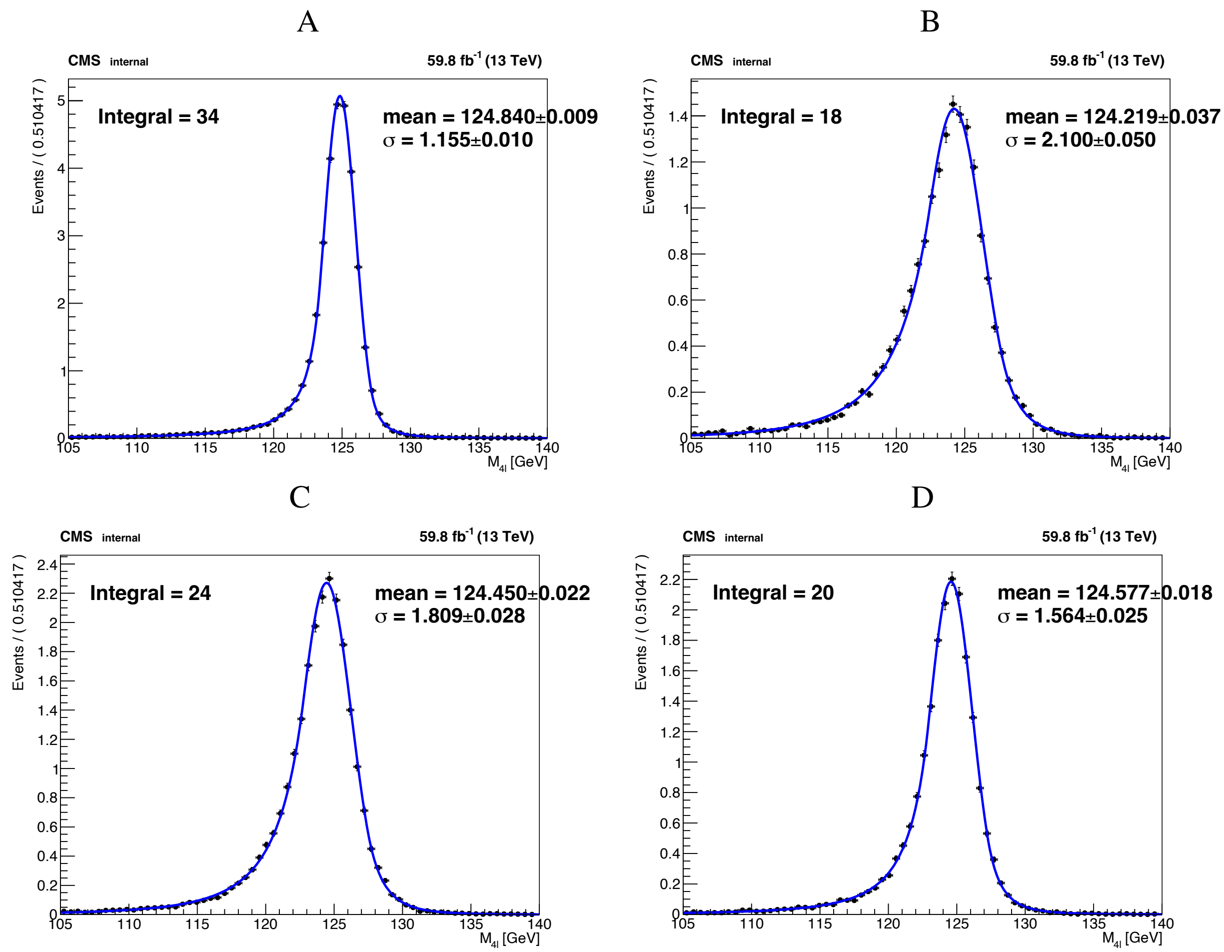

Figure 1-5. Four-lepton invariant mass distribution in the signal region ([105–140] GeV) using ggH events, with the DSCB fit for 2018: 4μ (top left), 4e (top right), 2e2μ (bottom left), 2μ2e (bottom right).

REFERENCES

[1] PARTICLE DATA GROUP collaboration, *Review of particle physics*, *Progress of Theoretical and Experimental Physics* **2020** (2020) 083C01.

BIOGRAPHICAL SKETCH

Jake Rosenzweig had the best childhood anyone could ask for, growing up in Jacksonville, FL: enjoying video games with excellent friends, playing football on the beach, and having plenty of opportunity to make mistakes. He graduated from the University of Florida in 2011 with a B.S. in chemistry, while maintaining his sanity by getting minors in education and Latin. He enjoys building things from scrap, weightlifting, hiking in the Coloradoan mountains, gardening, silence, and—most of all—receiving the beleaguered stare from his wife after telling her a *particularly* bad dad joke.